

The exponential convergence factors ensure the absolute convergence of the two infinite sums over n_3 and m_3 . Hence, the order of these sums is immaterial. Summing first over n_3 and σ , we may safely set $\eta_3=0$, for the series is convergent. Hence, we obtain

$$S(\epsilon_3, 0) = \sum_{\pi=1}^{3s} \sum_{m_3=0}^{\infty} e^{-\epsilon_3 m_3} [u_{\pi}(m_3; \omega'^2, \mathbf{k}_{\rho})]^* \times [\omega^2 u_{\pi}(m_3; \omega^2, \mathbf{k}_{\rho})]. \quad (\text{A3})$$

Similarly, if we sum first over m_3 and π , we obtain

$$S(0, \eta_3) = \sum_{\sigma=1}^{3s} \sum_{n_3=0}^{\infty} e^{-\eta_3 n_3} u_{\sigma}(n_3; \omega^2, \mathbf{k}_{\rho}) \times [\omega'^2 u_{\sigma}(n_3; \omega'^2, \mathbf{k}_{\rho})]^*, \quad (\text{A4})$$

but the dummy variable η_3, n_3, σ can clearly be replaced by ϵ_3, m_3, π . Furthermore, ω'^2 is real. Hence, Eq. (A4) reduces to

$$S(0, \epsilon_3) = \omega'^2 \sum_{\pi=1}^{3s} \sum_{m_3=0}^{\infty} e^{-\epsilon_3 m_3} [u_{\pi}(m_3; \omega'^2, \mathbf{k}_{\rho})]^* \times u_{\pi}(m_3; \omega^2, \mathbf{k}_{\rho}). \quad (\text{A5})$$

On the other hand, we can check directly that we require in (A1) only one convergence factor. That is,

$$S(\epsilon_3, \eta_3) = S(\epsilon_3, 0) = S(0, \epsilon_3). \quad (\text{A6})$$

Hence subtracting Eq. (A.3) from Eq. (A.4), we obtain

$$0 = (\omega'^2 - \omega^2) \sum_{\pi=1}^{3s} \sum_{m_3=0}^{\infty} e^{-\epsilon_3 m_3} [u_{\pi}(m_3; \omega'^2, \mathbf{k}_{\rho})]^* \times u_{\pi}(m_3; \omega^2, \mathbf{k}_{\rho}) \quad (\text{A7})$$

or

$$\sum_{\pi=1}^{3s} \sum_{m_3=0}^{\infty} e^{-\epsilon_3 m_3} [u_{\pi}(m_3; \omega'^2, \mathbf{k}_{\rho})]^* u_{\pi}(m_3; \omega^2, \mathbf{k}_{\rho}) = 0 \quad (\text{A8})$$

if $\omega^2 \neq \omega'^2$,

and, since ϵ_3 is arbitrary, we can now go to the limit $\epsilon_3 \rightarrow 0^+$. This proves Eq. (4.17) for $\omega^2 \neq \omega'^2$. A similar analysis leads to the proof of the Dirac delta-function normalization indicated in Eq. (4.17). We note here that the entire limiting procedure can be dispensed with when \mathbf{u} is a surface mode, for then the u 's themselves are exponentially bounded.

Current Saturation and Trap-Controlled Electron Drift Mobility in Photoconductive CdS[†]

ANDREAS RANNESTAD

Norwegian Defence Research Establishment, Kjeller, Norway

(Received 26 October 1965; revised manuscript received 14 November 1966)

Current saturation due to acoustic oscillations in CdS is observed, both in a transverse mode and in a longitudinal mode. The most pronounced saturation occurred in the transverse mode, although the applied dc field was parallel to the c axis, and one should expect saturation mainly in the longitudinal mode. A method for determining the threshold field for oscillation, utilizing the buildup time for current saturation under applied pulsed dc electric field, is discussed. The threshold field is used to determine the electron drift mobility for photoconducting CdS in the temperature range from 204 to 438°K. The temperature dependence of the mobility can be described as a combination of scattering from lattice vibration and trapping from two impurity levels, $\epsilon_1=0.02$ eV with density $N_1=6 \times 10^{17}$ cm⁻³ and $\epsilon_2=0.1$ eV with density $N_2=8 \times 10^{16}$ cm⁻³, and is given by

$$\mu_d = \frac{1.28 \times 10^6 T^{-3/2}}{1 + 1420 T^{-3/2} \rho^{0.02/kT} + 189 T^{-3/2} \rho^{0.1/kT}} \text{ cm}^2/\text{V sec.}$$

I. INTRODUCTION

IN their theoretical analysis of acoustoelectric amplification in piezoelectric semiconductors, Hutson and White^{1,2} indicated that trapped charge could have a large influence on the propagation constants, but made no use of this concept in their experimental verification of acoustoelectric amplification in CdS.³ Several authors⁴⁻⁶

have ignored this effect, while others have given the effect an extensive treatment.⁷⁻¹⁰ Moore and Smith⁹ have considered the effect of traps on acoustoelectric current saturation in CdS, and have shown that the

[†] Research sponsored by the Cambridge Research Laboratories under Contracts No. AF 61(052)-484 and -958 through the European Office of Aerospace Research, OAR, U. S. Air Force.

¹ A. R. Hutson and D. L. White, *J. Appl. Phys.* **33**, 40 (1962).

² D. L. White, *J. Appl. Phys.* **33**, 2547 (1962).

³ A. R. Hutson, J. H. McFee, and D. L. White, *Phys. Rev. Letters* **7**, 237 (1961).

⁴ H. N. Spector, *Phys. Rev.* **127**, 1084 (1962); **130**, 910 (1963).

⁵ S. G. Eckstein, *Phys. Rev.* **131**, 1087 (1963).

⁶ K. Bløtekjaer and C. F. Quate, *Proc. IEEE* **52**, 360 (1964).

⁷ I. Uchida, T. Ishiguro, Y. Sasaki, and T. Suzuki, *J. Phys. Soc. Japan* **19**, 674 (1964).

⁸ T. Ishiguro, I. Uchida, T. Suzuki, and Y. Sasaki, *IEEE Trans. SU-12*, 9 (1965).

⁹ A. R. Moore and R. W. Smith, *Phys. Rev.* **138**, A1250 (1965).

¹⁰ P. D. Southgate and H. N. Spector, *J. Appl. Phys.* **36**, 3728 (1965).

trapping effects are temperature-dependent and have a large influence on the electron drift mobility.

Acoustic waves are reflected at the ends of a crystal, and a piezoelectric semiconductor may therefore break into self-sustained acoustic oscillations if the round-trip gain exceeds unity. These oscillations give rise to current saturation and deviation from Ohm's law. Several authors^{9,11-16} have used this deviation in the current-voltage (I - V) characteristic to determine the electron drift mobility in CdS crystals.

There is some discrepancy in the literature with respect to the sound velocity to be used in calculating the electron drift mobility from saturation measurements. Smith¹¹ and Moore¹³ found the same threshold voltages for semiconducting samples with the electric field parallel ($\mathbf{E}||c$) and perpendicular ($\mathbf{E}\perp c$) to the hexagonal axis, and used the longitudinal sound velocity in their calculations, because this gave the most reasonable drift mobility. McFee¹² also found the same threshold voltage for saturation in photoconducting samples with $\mathbf{E}||c$ and $\mathbf{E}\perp c$; however, he found that the sample with $\mathbf{E}||c$ needed a much larger voltage for amplification of an external acoustic signal. He concluded that both sample types oscillated in the transverse mode, and that the saturation in the longitudinal-wave sample is brought about by the amplification of shear waves whose wave vector makes a finite angle with the hexagonal axis.

In the present experiment, the electric field was parallel to the c axis and we would expect oscillations in the longitudinal mode. By observing the transient behavior of current pulses we were able to show that two distinct modes of oscillation occurred. Comparison of the threshold voltages for these two modes with the threshold voltage for amplification of longitudinal waves, as obtained from an auxiliary acoustic-amplifier experiment, led to the conclusion that the lower voltage saturation is caused by shear-wave amplification, and that also longitudinal oscillations occur at higher voltages. Thus, our experiments strongly support McFee's conclusions.¹² Since the longitudinal-wave saturation took place only in a limited temperature range, the threshold voltage for the more pronounced shear-wave saturation, and hence the transverse sound velocity, was used to determine the trap-controlled electron drift mobility as a function of temperature.

II. EXPERIMENTAL APPARATUS AND TECHNIQUES

A. Sample

The CdS sample used in this experiment was cut from a photoconducting Eagle-Picher boule single crystal

with a dark resistivity of approximately 30 k Ω cm. The crystal was oriented such that the electric field was parallel to the hexagonal axis of symmetry. Evaporated indium contacts were applied to the optically flat end planes. The sample length was 1.21 mm, and the cross-sectional area was approximately 10 mm².

B. Apparatus

The CdS crystal was placed in a reservoir filled with isopropanol for low-temperature measurements and silicon oil for high-temperature measurements, in order to ensure constant temperature during measurements. The reservoir was placed in a Dewar system with liquid nitrogen as coolant in the outer Dewar and gaseous nitrogen as heat exchanger in the inner Dewar. The temperature was varied by means of a heating coil in the reservoir and measured with a thermocouple. The voltage pulses were supplied by a variable pulse generator and amplified by a pulse amplifier. The current pulses were monitored by means of an inductive current pickup and oscilloscope.

C. Experimental Method

A CdS crystal may break into self-sustained acoustic oscillations if the round-trip gain of an acoustic wave exceeds unity. The acoustoelectric current associated with the oscillations subtracts from the applied current, causing deviation from Ohm's law. A necessary requirement for acoustic amplification is that the electron drift velocity exceeds the phase velocity of the acoustic wave. Hence, the applied drift field must exceed a certain threshold before oscillation starts. If we observe the transients, as a drift field above the threshold value is switched on, we find that the initial current is in accordance with Ohm's law. After a time τ , the current starts decreasing to a lower level. τ is the time it takes for the acoustic flux to build up in the crystal; it should therefore be inversely proportional to the acoustic gain. Experimental curves for $1/\tau$ versus drift field resemble qualitatively the theoretical curves for the round-trip gain, and the threshold value of the drift field is given by the intersection of the $1/\tau$ -versus-drift-field curve with the field axis. The round-trip gain is determined by the gain of the forward wave, the attenuation of the backward wave, the internal losses, and the reflection losses; however, as a first approximation, only the gain of the forward wave and the attenuation of the backward wave need be considered. At zero gain, this leads to the well-known relationship⁶

$$(v_d/v_s)^2 = 1 + 4\omega_c/\omega_D = (\mu_d E_{th}/v_s)^2, \quad (1)$$

where v_d is the drift velocity of the electrons; μ_d is the drift mobility of the electrons; v_s is the phase velocity of the acoustic wave; $\omega_c = \sigma/\epsilon$ is the conductivity relaxation frequency; $\omega_D = v_s^2/D_n = v_s^2 e/\mu_d kT$ is the diffusion frequency; σ is the conductivity; ϵ is the dielectric constant; D_n is the electron diffusion constant; e is the electron charge; k is the Boltzmann constant; T is

¹¹ R. W. Smith, Phys. Rev. Letters **9**, 87 (1962).

¹² J. H. McFee, J. Appl. Phys. **34**, 1548 (1963).

¹³ A. R. Moore, Phys. Rev. Letters **12**, 47 (1964).

¹⁴ C. Hamaguchi, T. Otsuki, and Y. Inuishi, J. Appl. Phys. (Japan) **3**, 491 (1964).

¹⁵ C. Hamaguchi, T. Otsuki, Y. Watanabe, and Y. Inuishi, J. Appl. Phys. (Japan) **3**, 492 (1964).

¹⁶ A. Ishida, C. Hamaguchi, and Y. Inuishi, J. Phys. Soc. Japan **20**, 1946 (1965).

the temperature in °K; and E_{th} is the threshold field. This gives the following value for the drift mobility:

$$\mu_d = \frac{v_s}{E_{th}} \left(1 + 4 \frac{\omega_c}{\omega_D}\right)^{1/2} = \frac{v_s}{E_{th}} \left(1 + 4 \frac{\omega_c kT}{v_s^2 e}\right)^{1/2}. \quad (2a)$$

Rearranging and substituting appropriate values for CdS, one has

$$\mu_{d,l} = \frac{4.42 \times 10^5}{E_{th,l}} \left\{ \frac{4.8 \times 10^2 \sigma T}{E_{th,l}} + \left[\left(\frac{4.8 \times 10^2 \sigma T}{E_{th,l}} \right)^2 + 1 \right]^{1/2} \right\}, \quad (2b)$$

$$\mu_{d,t} = \frac{1.75 \times 10^5}{E_{th,t}} \left\{ \frac{1.17 \times 10^3 \sigma T}{E_{th,t}} + \left[\left(\frac{1.17 \times 10^3 \sigma T}{E_{th,t}} \right)^2 + 1 \right]^{1/2} \right\}, \quad (2c)$$

where the subscripts l and t refer to saturation caused by longitudinal and transverse sound waves, respectively.

We shall consider some possible sources of error. In addition to the attenuation in the backward direction, which is included in Eq. (2), there are also reflection losses and internal losses. The reflection losses were made small by making the end planes highly reflecting, and the internal losses are small. Thus these losses have little influence on the result when the measurements are performed with high acoustic gain in the crystal. However, these losses may have a relatively large influence at low acoustic gain.

Another source of error is a possible inhomogeneous field distribution in the sample. Part of the voltage falls across a narrow boundary layer, and there may also be an inhomogeneous field distribution within the crystal itself. However, the sample used in this experiment has a very linear current-voltage characteristic below the threshold voltage, such that the neglect of inhomogeneities is believed to have little influence on

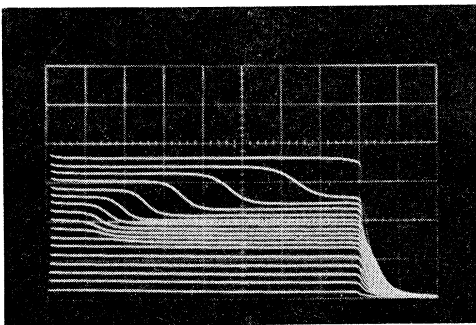


FIG. 1. Typical current pulses for varying voltage (100–1700 V). Time scale 10 μ sec per major division, current scale 100 mA per major division, and sample temperature 258°K.

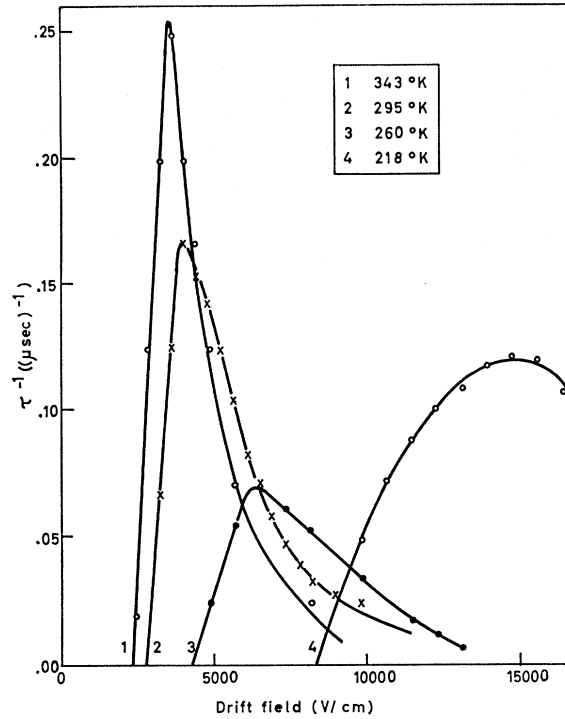


FIG. 2. $1/\tau$ versus applied electric field for different temperatures. Sample conductivity = 3×10^{-4} (Ω cm) $^{-1}$.

the results. Electro-optical measurements also indicate a nearly homogeneous field distribution in CdS crystals before saturation occurs.¹⁷ An important source of error is the phase velocity used in Eq. (2c). Since the transverse waves propagate at an angle with respect to the drift field ($E \parallel c$ axis), a phase velocity in excess of 1.75×10^5 cm/sec should be used when calculating the electron drift mobility. The experimental measurements indicate a 10% increase, but since the phase velocity could not be determined accurately the above given value was used. It should be emphasized that the sources of errors discussed all act in the same direction, and the result is an absolute lower bound for the mobility.

III. RESULTS AND INTERPRETATION

Figure 1 shows a typical picture of the current pulses for applied voltages from the lowest trace 100 to 1700 V in 100 V steps. The temperature of the sample was 258°K, the time scale 10 μ sec per major division, and the current scale 100 mA per major division. The picture clearly shows how the time for the onset of saturation changes with applied voltage. As the voltage increases, the time τ decreases, goes through a minimum, and then starts to increase.

Figure 2 shows some typical plots of $1/\tau$ versus applied field. The plots show that the field required for

¹⁷ H. J. Fossum, Norwegian Defense Research Establishment Scientific Report No. 2, Contract No. AF61(052)-958 (unpublished).

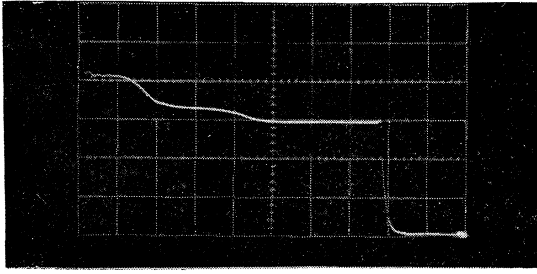


FIG. 3. Typical current pulse for double saturation (1300 V). Time scale 10 μ sec per major division and sample at room temperature.

the onset of saturation increases as the temperature is lowered from 343 to 218°K, while the curves steadily broaden. This is in accordance with theory. The plots also indicate that for decreasing temperature, the maximum gain decreases, goes through a minimum, and then starts to increase. Assuming that we have maximum amplification for the angular frequency $\omega = (\omega_c \omega_D)^{1/2}$ and neglecting the effects from trapping and the reflected wave, we find that the maximum in gain should be proportional to $(\mu_d T)^{-1/2}$. We would therefore expect the minimum gain point to be at a higher temperature than that for maximum electron drift mobility, while in the present case we see that the minimum gain point is shifted to a lower temperature. No adequate explanation has been found for this shift in the minimum gain point. At higher temperatures, double current saturation was observed. A typical picture of the current pulse under conditions for double saturation is shown in Fig. 3. The picture was taken with a pulse voltage at 1300 V, the time scale is 10 μ sec per major division, and the sample was at room temperature. Figure 4 gives $1/\tau$ versus applied electric field for double saturation. The sample temperature was 343°K and the conductivity approximately 3×10^{-4} (Ω cm) $^{-1}$. Assuming that the low-voltage saturation is due to a transverse mode and the high-voltage saturation is due to a longitudinal mode, we obtain the following electron drift mobilities from Eqs. (2b) and (2c):

$$\mu_{d,t} = 79 \text{ cm}^2/\text{V sec}, \text{ and } \mu_{d,l} = 88 \text{ cm}^2/\text{V sec}.$$

This is a good indication that our assumptions are correct. Other experiments at this laboratory have shown similar results.¹⁸ For a further verification of our assumptions, we placed the sample in an experimental acoustoelectric amplifier for longitudinal waves, and found the point of zero gain at 780 V, while we noticed saturation in the crystal at much lower voltages. This threshold voltage gives an electron drift mobility of $\mu_{d,l} = 70 \text{ cm}^2/\text{V sec}$ which is in good agreement with the drift mobility found by the saturation method at room temperature. In view of the above experimental findings, we concluded that the main saturation was in the trans-

verse mode, and the second saturation in the longitudinal mode. Figure 4 shows that the total gain is considerably higher in the transverse mode than in the longitudinal mode. The higher gain for shear-wave amplification usually suppressed the longitudinal oscillations to the extent that these were not observed.

Using the experimental values of the threshold field obtained from the $1/\tau$ versus applied field curves in Eq. (2c), we obtain the electron drift mobilities plotted in Fig. 5.

The low experimental values for the electron drift mobility are assumed to be due to extensive trapping in the crystal. From a simple model with discrete trapping levels we get the following general expressions for the temperature dependence of the drift mobility¹⁹:

$$\mu_d = \mu_e \frac{n}{n+n_t} = \mu_e \left(1 + \frac{1}{N_c} \sum_t N_t e^{\epsilon_t/kT} \right)^{-1}, \quad (3)$$

where n is the number of free electrons; n_t is the number of trapped electrons; μ_e is the electron drift mobility without trapping; N_c is the effective density of states in the conduction band; N_t is the density of trapping levels; and ϵ_t is the energy difference between the bottom of the conduction band and the trapping level.

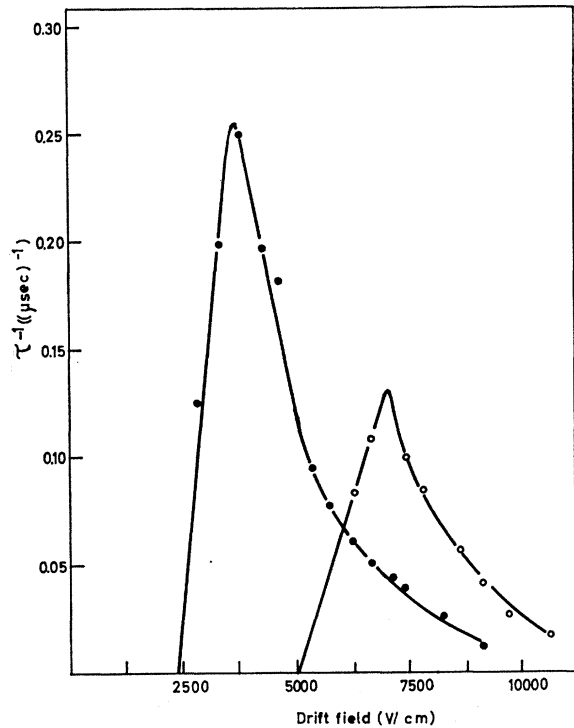


FIG. 4. $1/\tau$ versus applied electric field for double saturation. Sample temperature-343°K and conductivity= 3×10^{-4} (Ω cm) $^{-1}$.

¹⁸ L. O. Svaasand, Norwegian Defense Research Establishment Scientific Report No. 12, Contract No. AF61(052)-484 (unpublished).

¹⁹ A. Rannestad, Norwegian Defense Research Establishment Scientific Report No. 1, Contract No. AF61(0.52)-958 (unpublished).

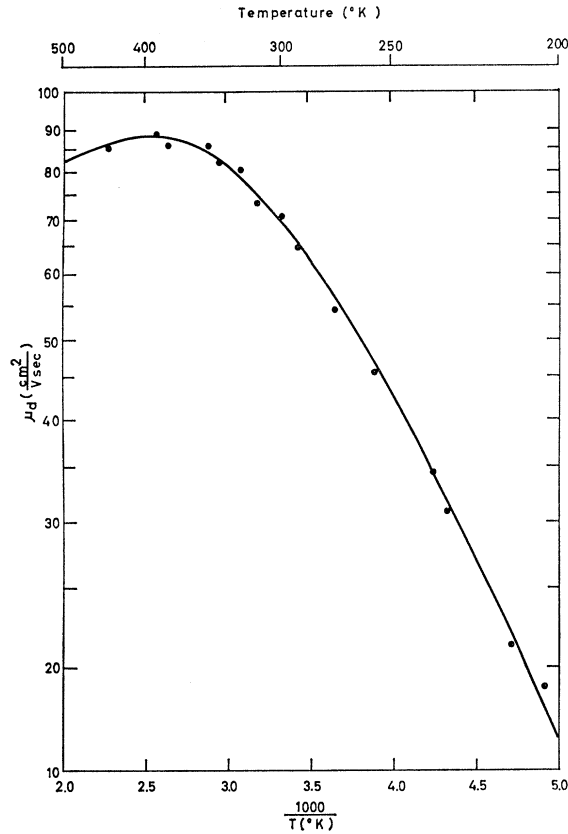


FIG. 5. Temperature dependence of electron drift mobility. The solid line is the theoretical curve with parameters chosen to fit the experimental points. Sample conductivity = 5×10^{-4} (Ω cm) $^{-1}$.

This equation is essentially the same as the one used by Spear and Mort²⁰ and Moore and Smith.⁹ Spear and Mort²⁰ and Bradberry and Spear²¹ measured the electron drift mobility by studying the charge transport in CdS crystals, and found that the electron mobility due to lattice scattering was given by²⁰

$$\mu_L = 1.28 \times 10^6 T^{-3/2} \text{ cm}^2/\text{V sec}. \quad (4)$$

They also found that high-mobility CdS crystals have a shallow trapping level with activation energy that decreases with increasing trap density, and the energy is given by²⁰

$$\epsilon_i = \epsilon_0 - aN_i^{1/3}, \quad (5)$$

where

$$\begin{aligned} \epsilon_0 &= 0.049 \text{ eV}, \\ a &= 4.2 \times 10^{-8} \text{ eV cm}. \end{aligned}$$

Neglecting impurity scattering and inserting the values given in Eqs. (4) and (5) into Eq. (3), a good fit with

²⁰ W. E. Spear and J. Mort, Proc. Phys. Soc. (London) **81**, 130 (1963).

²¹ G. W. Bardberry and W. E. Spear, J. Appl. Phys. Britain **15**, 1127 (1964).

the experimental values was found by assuming two trapping levels: a shallow level at $\epsilon_1 = 0.02$ eV with a density $N_1 = 6 \times 10^{17}$ cm $^{-3}$, and a deep level at $\epsilon_2 = 0.1$ eV with a density $N_2 = 8 \times 10^{16}$ cm $^{-3}$. The electron drift mobility is then given by

$$\mu_d = \frac{1.28 \times 10^6 T^{-3/2}}{1 + 1420 T^{-3/2} e^{0.02/kT} + 189 T^{-3/2} e^{0.1/kT}} \text{ cm}^2/\text{V sec}, \quad (6)$$

which is plotted in Fig. 5.

It should be noted that the most critical parameter in Eq. (6) is ϵ_2 . A change in ϵ_2 from 0.1 eV to 0.11 eV will cause a change in the value for the electron drift mobility from 16 to 7.5 cm 2 /V sec at 200°K. The influence decreases with increasing temperature and is reduced to about 20% at room temperature. A 10% change in N_2 will cause about a 10% change in the drift mobility at 200°K. This influence is reduced to about half at room temperature. A 10% change in ϵ_1 with the appropriate change in N_1 will have considerably less influence on the drift mobility.

IV. DISCUSSION

The upper bound for the trap-controlled electron drift mobility is given by the lattice mobility. Since the sources of errors in measuring the mobility by acousto-electric saturation, such as neglect to consider the backward attenuation, reflection losses, and inhomogeneous field distribution, all act in the same direction such that the experimental results are an absolute lower bound for the mobility, the experimental measurements of the electron drift mobility should not exceed the lattice mobility. Spear and Mort²⁰ found the lattice mobility given in Eq. (4), and this is in good agreement with the data obtained by Kröger *et al.*²² and Miyazawa *et al.*,²³ while Piper and Halsted²⁴ found the lattice mobility to be about 50% higher. The lattice mobility given in Eq. (4) is used in this paper.

In comparing the earlier measured trap-controlled electron drift mobilities with the given lattice mobility, one finds that most experimental results obtained by using the saturation method give a drift mobility higher than the lattice mobility of Eq. (4) at high temperatures.^{11,13-16} If one includes the contribution of the backward attenuation, this is even more pronounced. Since the lattice mobility should be the upper bound for the electron drift mobility and the results of McFee¹² as well as of the present experiment show that the transverse mode may give the strongest saturation, it seems most likely that the saturation was due to trans-

²² F. A. Kröger, H. J. Vink, and J. Volger, Physica **20**, 1095 (1954).

²³ H. Miyazawa, H. Maeda, and H. Tomishima, J. Phys. Soc. Japan **14**, 41 (1959).

²⁴ W. W. Piper and R. E. Halsted, in *Proceedings of the International Conference on Semiconductor Physics, Prague, 1960* (Academic Press Inc., New York, 1961), p. 1046.

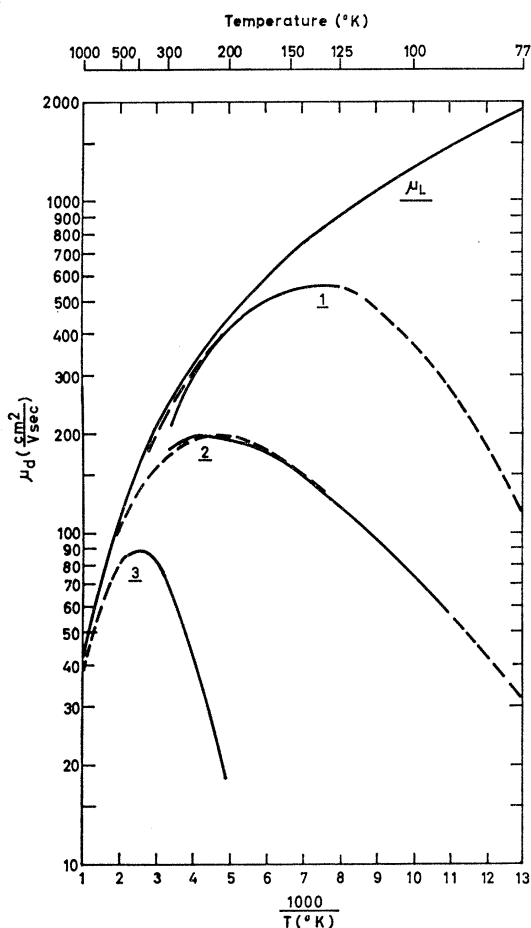


FIG. 6. Temperature dependence of electron drift mobility, comparison with earlier experiments. μ_L , lattice mobility (Ref. 20); 1, Ishida *et al.* (Ref. 16); 2, Moore and Smith (Ref. 9); and 3, present experiment. (See text for further explanations.)

verse acoustic waves also in the experiments referred to above.

In order to compare the earlier results with the present results and to see how they fit into the simple trapping model given in Eq. (6), the data obtained by Ishida *et al.*¹⁶ and the data obtained by Moore and Smith⁹ for the photoconducting sample were recalculated, using Eq. (2c), and plotted in Fig. 6. The solid lines come from the measured data, while the dashed lines are calculated from Eq. (6). In Fig. 6, the following symbols are used: μ_L , lattice mobility from Eq. (4); curve 1, Ishida *et al.*,¹⁶ $\sigma = 10^{-3}$ and $\epsilon_1 = 0.04$ eV with $N_1 = 9 \times 10^{15}$ cm^{-3} ; curve 2, Moore and Smith,⁹ σ assumed 10^{-3} and

$\epsilon_1 = 0.025$ eV with $N_1 = 3.5 \times 10^{17}$ cm^{-3} ; and curve 3, the data presented in Fig. 5. Figure 6 shows that the data fit very well with the simple trapping model and are in good agreement with the empirical relation between the shallow trapping level and the trap density found by Spear and Mort²⁰ and given by Eq. (5).

Bradberry and Spear,²¹ in low-mobility crystals, mainly in boule crystals made by Eagle-Picher, found that the electron drift mobility was controlled by a deep trapping level at 0.15–0.16 eV. The crystal used in the present experiment had an intermediate mobility and indicated a deep trapping level at 0.1 eV. The difference in the energy of the deep trapping level found in the two experiments could indicate that there exist several trapping levels, but a verification of this can only be found by further experiments.

V. SUMMARY AND CONCLUSIONS

The present experiment clearly shows that one may obtain current saturation because of amplification of both transverse and longitudinal acoustic waves in a longitudinal-wave photoconducting CdS sample, and that the gain in the transverse mode may be larger than the gain in the longitudinal mode. It is shown that the data obtained by Ishida *et al.*¹⁶ and Moore and Smith⁹ for photoconducting CdS samples lie below the upper limit given by the lattice mobility if one assumes saturation in the transverse mode, while they exceed this limit at higher temperatures if one assumes saturation in the longitudinal mode. We conclude that the saturation is more pronounced in the transverse mode, and suggest that the samples used by other authors^{9,11,13–16} have oscillated in a transverse mode.

The experimental values of the electron drift mobility fit well with a simple model using two trapping levels: a shallow trapping level, which is in good agreement with the findings of Spear and Mort,²⁰ the data of Ishida *et al.*¹⁶ and of Moore and Smith,⁹ and a deep trapping level with an energy of about $\frac{2}{3}$ of that found by Bradberry and Spear²¹ for a very low-mobility sample. From these observations, one may conclude that the electron drift mobility is trap controlled and that there exist at least two trapping levels.

ACKNOWLEDGMENTS

The author thanks his colleagues at the Norwegian Defence Research Establishment for cooperation in carrying out this research. Special thanks are due Dr. K. Bløtekjaer.

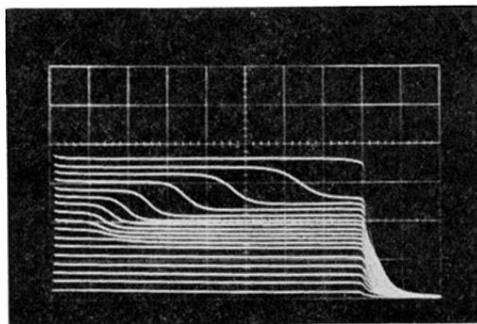


FIG. 1. Typical current pulses for varying voltage (100–1700 V). Time scale 10 μ sec per major division, current scale 100 mA per major division, and sample temperature 258°K.

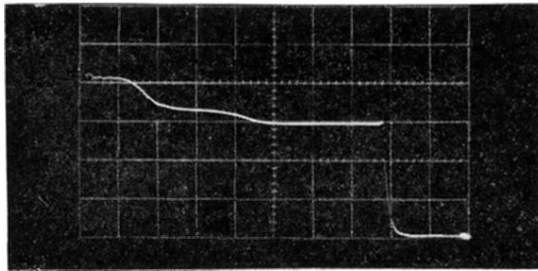


FIG. 3. Typical current pulse for double saturation (1300 V). Time scale 10 μ sec per major division and sample at room temperature.